AD-A248 090

SHOCK TUBE SIMULATION BY THE
SMOOTH PARTICLE HYDRODYNAMIC
(SPH) METHOD

THESIS

Luke A. Lorang, Captain, USAF

AFIT/GNE/ENP/92M-6

92-08121

DEPARTMENT OF THE AIR FORCE
AIR UNIVERSITY

AIR FORCE INSTITUTE OF TECHNOLOGY

Wright-Patterson Air Force Base, Ohio

92 3 31 069

AFIT/GNE/ENP/92M-6

SHOCK TUBE SIMULATION BY THE
SMOOTH PARTICLE HYDRODYNAMIC
(SPH) METHOD

THESIS

Luke A. Lorang, Captain, USAF

AFIT/GNE/ENP/92M-6

REPORT DOCUMENTATION PAGE

Form Approved
OMB No. 0704-0188

1. AGENCY USE ONLY (Leave blank)	2. REPORT DATE March 1992	3. REPORT TYPE AND DATES COVERED Master's Thesis

4. TITLE AND SUBTITLE
SHOCK SIMULATION BY THE
SMOOTH PARTICLE HYDRODYNAMIC
(SPH) METHOD

5. FUNDING NUMBERS

6. AUTHOR(S)

Luke A. Lorang, Capt, USAF

7. PERFORMING ORGANIZATION NAME(S) AND ADDRESS(ES)

Air Force Institute of Technology
WPAFB OH 45433-6583

8. PERFORMING ORGANIZATION REPORT NUMBER

AFIT/GNE/ENP/92M-6

9. SPONSORING/MONITORING AGENCY NAME(S) AND ADDRESS(ES)

Approved for public release; distribution
unlimited

10. SPONSORING/MONITORING AGENCY REPORT NUMBER

11. SUPPLEMENTARY NOTES

12a. DISTRIBUTION/AVAILABILITY STATEMENT

12b. DISTRIBUTION CODE

13. ABSTRACT (Maximum 200 words)

A smooth particle hydrodynamic code (SPHC) is evaluated for performing shock wave simulations by application to 1-D shock tube problems. Results of a shock tube test case with a compression ratio of 10 are compared against a Riemann shock tube problem and theoretical predictions of shock tube behavior to validate the SPH code. A Lagrangian hydrodynamic code is validated in a similar fashion. The resolution capabilities of both codes are compared using 100, 200 and 500 particles for SPHC and 100, 400 and 800 cells for the Lagrangian code. The SPH code exhibits a sharp spike in density at the contact discontinuity for a shock tube test case run with a compression ratio of 100. This behavior is not reported in the literature and not seen in the Lagrangian code results. Run time scaling is investigated for both codes. SPHC is found to scale between $N \log N$ and N^2, where N is the number of particles. The Lagrangian code scales $O(N^2)$. Computation times for the SPH code are greater than run times for the Lagrangian code by a factor of four for $N \leq 500$ to achieve similar resolution.

14. SUBJECT TERMS
Smooth Particle Hydrodynamics, SPH Schemes, Shock Tubes
Lagrangian Hydrodynamics

15. NUMBER OF PAGES
48

16. PRICE CODE

17. SECURITY CLASSIFICATION OF REPORT Unclassified	18. SECURITY CLASSIFICATION OF THIS PAGE Unclassified	19. SECURITY CLASSIFICATION OF ABSTRACT Unclassified	20. LIMITATION OF ABSTRACT UL

SHOCK TUBE SIMULATION BY THE

SMOOTH PARTICLE HYDRODYNAMIC

(SPH) METHOD

THESIS

Presented to the Faculty of the School of Engineering

of the Air Force Institute of Technology

Air University

In Partial Fulfillment of the

Requirements for the Degree of

Master of Science in Nuclear Engineering

Luke A. Lorang, B.S.

Captain, USAF

March 1992

Approved for public release; distribution unlimited

Preface

The purpose of this study was to evaluate the smooth particle hydrodynamic (SPH) method and establish its credibility as a tool for shock wave simulation. SPH is a relatively recent numerical method and shows promise for 2- and 3-dimensional computations of gas-dynamical flows.

Evaluation of the SPH code was limited to one-dimensional shock tube problems because it was the only version of the code available for study. Therefore, the code was validated against theoretical predictions of shock tube behavior and a standard Riemann shock tube solution. The SPH code was also compared to a Lagrangian hydrodynamic code. For similar resolution of shock tube density features, the SPH code proved to be computationally more expensive. It also displayed anomalous behavior at the contact discontinuity. This was only a preliminary evaluation and the full capability of the SPH method for shock wave simulation is still uncertain.

I gratefully acknowledge the support and guidance of my faculty advisor, LCDR Kirk Mathews. He demonstrated unexpected patience and understanding during the low points of my research effort.

<div align="right">Luke</div>

Table of Contents

List of Figures

List of Tables

v

Abstract

A smooth particle hydrodynamic code (SPHC) is evaluated for performing shock wave simulations by application to one-dimensional shock tube problems. Results of a shock tube test case with a compression ratio of 10 are compared against a standard Riemann shock tube problem and theoretical predictions of shock tube behavior to validate the SPH code. A Lagrangian hydrodynamic code is validated in a similar fashion. The resolution capabilities of both codes are compared using 100, 200 and 500 particles for SPHC and 100, 400 and 800 cells for the Lagrangian code. The SPH code exhibits a sharp spike in density at the contact discontinuity for a shock tube test case run with a compression ratio of 100. This behavior is not reported in the literature and not seen in the Lagrangian code results. Run time scaling is investigated for both codes. SPHC is found to scale between $N \log N$ and N^2, where N is the number of particles. The Lagrangian code scales $O(N^2)$. Computation times for the SPH code are greater than run times for the Lagrangian code by a factor of four for $N \leq 500$ to achieve similar resolution of shock tube features.

SHOCK TUBE SIMULATION BY THE

SMOOTH PARTICLE HYDRODYNAMIC

(SPH) METHOD

I. Introduction

Approximately 50 percent of the energy released by a fission weapon in air at moderate altitudes (40,000 ft) or lower contributes to production of a shock (or blast) wave (1:7). Most of the material damage resulting from the nuclear explosion is attributable to the blast wave. Blast wave phenomena, therefore, are of great interest in nuclear weapon effects and nuclear survivability studies. However, gaining experimental data of blast wave interaction with structures is extremely difficult. All aboveground testing of nuclear weapons in the United States ended with the nuclear weapons test-ban agreement of 1963 (2:273). Alternative methods, therefore, were developed. Air blast testing can be conducted in shock tubes, simulated using large high explosive (HE) charges, and performed computationally. The high cost of performing shock tube and HE testing limits the frequency and variety of that type of testing.

On the other hand, numerical simulation is a relatively inexpensive method for studying blast wave propagation in air

and blast loading of structures. Numerical hydrodynamic methods offer the benefits of low cost, unlimited parametric studies, flexibility of boundary configurations and conditions, and repeatability of results. Computational methods are not without their problems, though. Computation times increase dramatically for two- and three- dimensional shock problems. Traditional finite difference methods involving a spatial mesh suffer from mesh tangling or inaccuracies associated with the severe distortion of the mesh for multidimensional problems. Eulerian codes may require such fine meshing and short time steps to achieve desired resolution in the solution that computation time, and therefore cost, becomes prohibitive. Lastly, numerical solutions are only as good as the physics that goes into their formulation. Thus, new numerical methods that offer performance enhancements and increased accuracy over previous hydrodynamic codes are of great interest and merit evaluation. One of these new methods is smooth particle hydrodynamics (SPH).

1.1 SPH Background

Smooth particle hydrodynamics was developed for astrophysics applications involving fluid masses moving arbitrarily in three dimensions in the absence of boundaries. Lucy (3) first applied SPH to the problem of protostellar fission. Gingold and Monaghan (4) extended this work and also applied SPH to one-dimensional shock tube problems by incorporating an artificial viscosity into the equations of motion.

Experiments showed that this artificial viscosity term produced negligible oscillation and good resolution of the shock front and contact discontinuity (4:375). Recently, Benz has applied this technique to planetary (5) and stellar (6) collisions.

Particle methods are often computationally superior to mesh-based methods when computing highly asymmetric three-dimensional gas-dynamical flows (7:414). Highly distorted flows and large voids occur during impacts or mass transfer in stellar collisions. Lack of a mesh makes SPH particularly suited for simulating such problems since it does not risk mesh entanglement. Also, no memory or computational time is wasted by having a large number of empty cells just in case some material moves into them (8:649) as in Eulerian schemes.

Certain limitations of these methods have discouraged their application to non-astrophysical problems. One disadvantage of SPH is run time scaling. SPH particles interact with a variable number and set of neighboring particles which can lead to excessive computation (9). Another disadvantage is particle streaming between colliding fluid elements (10). This results in anomalous fluid interpenetration which does not occur in a real physical system. Also, for fixed mass particles, low density regions exhibit poor resolution due to the fewer particles in these regions relative to higher density ones. Lastly, SPH has no grid, and treatment of boundaries has been largely ignored until recently since they are not important in astrophysical applications.

Steilingwerf (11) reports that a new implementation of SPH by the Mission Research Corporation (MRC) overcomes the inherent disadvantages of SPH. This new SPH code, SPHC, has been tested by MRC against analytic solutions and other hydrodynamic codes on rarefaction, shock tube, blast wave and collision problems as well as reproducing laboratory results in laser/target experiments. It is this code which will be evaluated here.

1.2 Problem and Scope

The objective of this study is to evaluate the merits of the SPH method as a simulation tool for modeling blast wave phenomena in air from a nuclear explosion. The primary goal is to evaluate the computational performance of the SPH code in resolution capability and run-time scaling using a 1-D shock tube test case. The approach is to compare SPH shock tube results to a conventional (meshed) 1-D Lagrangian hydrodynamic code. A second goal is to apply SPH to a practical application such as the stagnation/amplification of a shock wave in a corner. Due to difficulties encountered using the SPH code, this second objective was not met.

1.3 Development

A theoretical development of the SPH method from the integral form to the particle approximation is presented in Section II. Section III provides details of the shock tube validation for the SPH and 1-D Lagrangian hydrodynamic codes. A comparison of the resolution capabilities and run time scaling

4

results of the two codes is detailed in Section IV. Section V presents an analysis of the SPH code such as its unique features and problem applications. Conclusions and recommendations are presented in section VI.

II. Theoretical Development of SPH

In this section a theoretical development of the SPH method is presented based on the references by Gingold and Monaghan (4,12).

2.1 Theory

SPH is a free Lagrangian method for solving the conservation equations of hydrodynamics by replacing the continuum of hydrodynamic variables with a finite number of points. SPH is a Lagrangian method in the sense that points move with the fluid. The velocity and thermal energy at these points are known at any time. A mass is assigned to each point, so they are referred to as particles. Values of continuous hydrodynamic variables such as density and pressure are defined by an appropriate average over the distribution of particle values using a special weighting function, the smoothing function (or interpolating kernel).

To represent a continuous flow variable at r by a smoothed local average over a distribution of particles, consider the kernel estimate of the function $f(r)$ in the domain D

$$f_\kappa(r) = \int_D f(r')W(r,r',h)dr' \qquad (1)$$

where

κ =   kernel estimate

r' =   position of a particle

$f(r')$ =   the function interpolated

W =   the interpolating kernel

The interpolating kernel has the following properties:

(a) $$\int_D W(r,r',h)\,dr' \rightarrow 1 \qquad \text{as} \quad h \rightarrow 0. \tag{2}$$

(b)   If $f(r)$ is a continuous function

$$f_\kappa(r) \rightarrow f(r) \qquad \text{as} \quad h \rightarrow 0. \tag{3}$$

Therefore, the interpolating kernel acts like a delta function, and it does so more closely as $h \rightarrow 0$. The smoothing length h is chosen so that it determines the extent to which W confines the major contribution to $f_\kappa(r)$ to the neighborhood of $r = r'$ (12:423).

Although there are many possible kernels to choose from, only two kernels are commonly used (6:616): the Gaussian and exponential kernels. The Gaussian kernel is given by

$$W(r,r',h) = \frac{\exp[-(r-r')^2/h^2]}{(\pi h^2)^{3/2}} \tag{4}$$

whereas the exponential kernel is given by

$$W(r,r',h) = \frac{\exp[-(|r-r'|)/h]}{8\pi h^3} \tag{5}$$

7

Assuming that we have a set of N points $r_1, r_2, \ldots, r_N$ distributed in space according to the number density $n(r)$, $f_\kappa(r)$ from Eq (1) can be approximated by

$$f_\kappa(r) = \sum_{j=1}^{N} \frac{f(r_j)}{n(r_j)} W(r, r_j, h) \qquad (6)$$

This expression for $f_\kappa(r)$ is the general SPH interpolation formula. The usual case for particle methods is to define the mass density $\rho(r)$ as

$$\rho(r) = m(r) n(r) \qquad (7)$$

where $m(r)$ is the mass of each particle. For most purposes it is assumed that $W(r, r_j, h) = W(|r - r_j|, h)$. Eq (6) then becomes

$$f_\kappa(r) = \sum_{j=1}^{N} f_j \frac{m_j}{\rho_j} W(|r - r_j|, h) \qquad (8)$$

where, for any function B, $B_j = B(r_j)$.

The gradient of a function is given by

$$\nabla f_\kappa(r) = \sum_{j=1}^{N} f_j \frac{m_j}{\rho_j} \nabla W(|r - r_j|, h) \qquad (9)$$

The next step in developing the SPH method is to construct equations suitable for numerical work. Each of the exact equations is multiplied by the interpolating kernel and then integrated over the domain where a solution is required. Integration by parts gives the equations for numerical work. Monaghan and Gingold (4) recommend simply dropping nonlinear boundary terms since the kernel should mimic a delta function which goes to zero sufficiently far from the particles rep-

8

resenting the edge of the system. However, if one is to consider problems where the particles interact with a boundary condition, such as an externally-applied pressure, one must specifically include the boundary terms (13:5). The SPH code evaluated in this study includes the nonlinear boundary terms and will be discussed in the following sections.

III. 1-D Shock Tube Validation

The equations governing fluid behavior, theoretical predictions of shock tube behavior and validation of the SPH and Lagrangian hydrodynamic codes are presented in this section.

3.1 Governing Equations

The basic mathematical model of the physical laws governing the motion of an ideal or inviscid fluid is the set of Euler equations. These equations of motion are derived by applying the principles of conservation of mass, momentum and energy to a differential volume of compressible fluid.

For most practical purposes, the conservation equations are expressed as a set of nonlinear partial differential equations (PDEs). The resulting three equations are functions of four variables which describe the fluid medium: pressure p, density ρ, fluid velocity $\vec{u}$, and the internal energy per unit mass e. Adding an equation of state of the form $e = f(p, \rho)$ completes the system of equations and allows for a solution. This system of equations describes the variations in fluid properties throughout time and space. Also, (assuming that pressures, velocities and temperatures change sufficiently slowly with distance) heat conduction, viscous and all other internal irreversible processes are neglected (14:6).

The Euler equations in conservation form for one dimension are:

$$\frac{\partial U}{\partial t} + \frac{\partial f(U)}{\partial x} = 0 \qquad (11)$$

where

$$U = \begin{bmatrix} \rho \\ \rho u \\ \rho e_t \end{bmatrix} \qquad\qquad f(U) = \begin{bmatrix} \rho u \\ \rho u^2 + p \\ \rho u(e_t + p/\rho) \end{bmatrix}$$

and e_t is the total energy per unit mass given as

$$e_t = e + \frac{u^2}{2} \qquad (12)$$

Internal energy is related to pressure by the equation of state for a perfect gas

$$p = (\gamma - 1)\rho e \qquad (13)$$

Calculating the flow properties across the shock front requires applying the Rankine-Hugoniot conditions for changes across a normal shock.

A shock tube can be modelled using these hyperbolic conservation equations, Eq (11), as a set of initial-value problems with piecewise constant initial data

$$U(x,0) = U_L \; (for \; x < 0); \quad U(x,0) = U_R \; (for \; x > 0) \qquad (14)$$

separated by a discontinuity at $x = 0$. This special initial-value problem is defined as a Riemann problem (15:357). The shock tube problem is a special Riemann problem with $u_L = u_R = 0$ (16:664). The Riemann shock tube problem has an

exact solution and thus provides a benchmark for approximate solutions. Figure 1 compares exact and approximate solutions to a Riemann problem for air with a density ratio of 8:1.
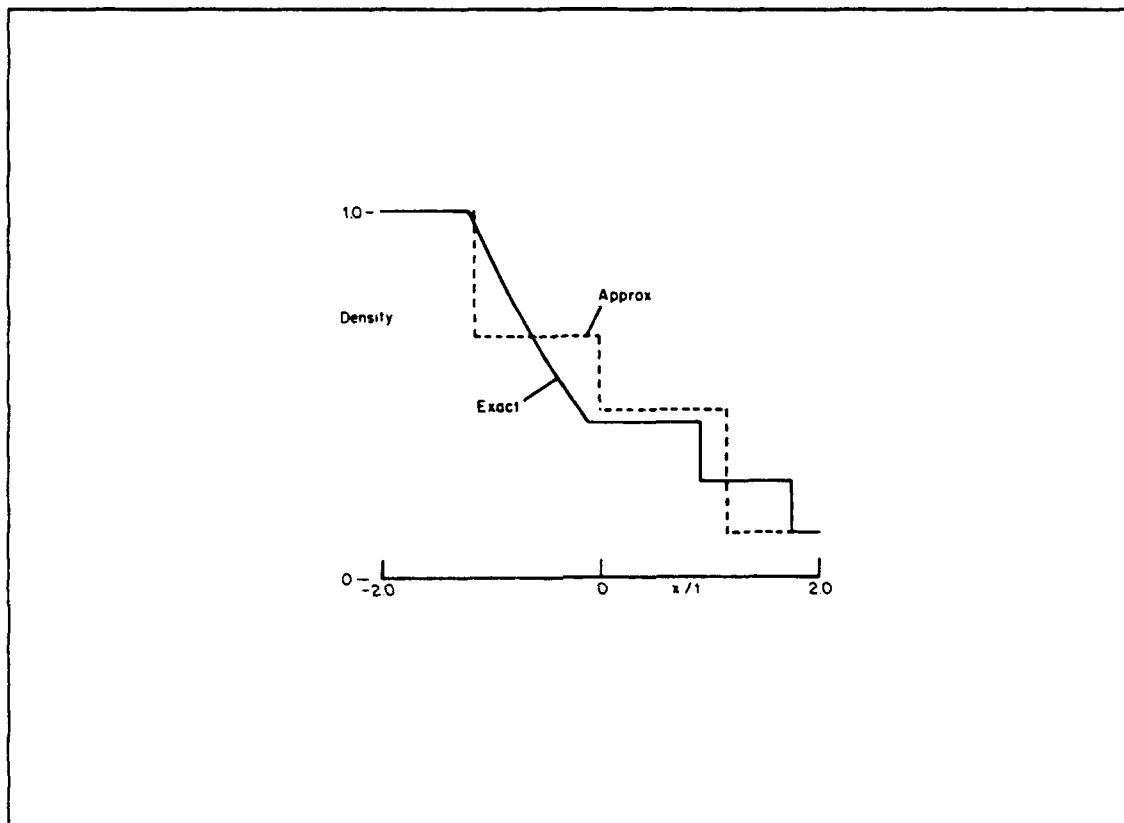

Figure 1.   Exact and Approximate Solutions to a Riemann Problem (15:368)

An algorithm for calculating approximate solutions to a Riemann problem was presented by Roe in Reference 15. However, the equations for the exact solution were not included; the algorithm for the exact solution was taken from Sod (17). Thus, Figure 1 only provides a qualitative example of the expected density profile in a shock tube for time $t > 0$.

12

3.2 Theoretical Predictions

Figure 2a shows a simple shock tube. A gas-tight diaphragm separates the shock tube into two sections. One-half of the tube, known as the compression chamber, contains the compressed gas at a pressure p_3, which is in excess of the pressure p_0 of the gas in the other half of the tube known as the expansion chamber.
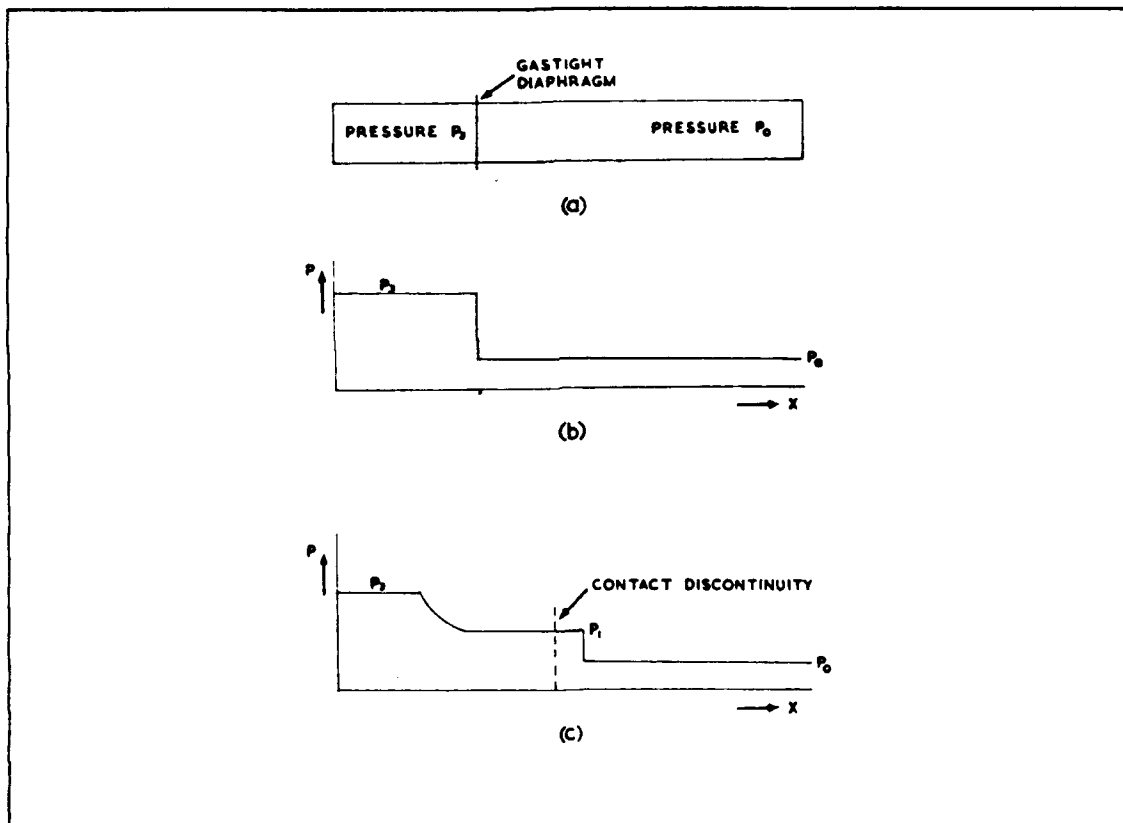

Figure 2. Shock Tube, a) assembly, b) pressure history at t = 0, c) t > 0 (14:29)

Upon shattering the diaphragm, a shock wave propagates into the expansion chamber while a rarefaction wave propagates

back into the compression chamber. Figures 2b and 2c show the pressure profile along the shock tube before and after the diaphragm has shattered. The dotted line in Figure 2c indicates the position occupied by that gas which was originally at the diaphragm. The gas to the right has been compressed and heated by the shock wave while the gas to the left of this line has expanded from the compression chamber and has therefore been cooled. This position is a contact discontinuity. At this point there will be a discontinuity in gas temperature and density. Pressure, however, remains constant across this discontinuity as seen in Figure 2c. If this were not the case, a shock front would form at this location as well. Velocity also remains constant across the contact discontinuity.

When the shock wave encounters the rigid wall at the end of the shock tube, it undergoes a reflection and will be reflected as a shock wave. Likewise the rarefaction wave travelling into the compression chamber also encounters a rigid wall and will be reflected as a rarefaction wave.

3.3   SPHC Shock Tube Validation

A 1-D shock tube test case was run with SPHC to provide confidence in its output. The program default parameters were used. Table 1 lists the initial conditions. It is assumed that the gas on both sides of the diaphragm are in thermal equilibrium and therefore are both at the same temperature.

The compression ratio η is defined as the ratio of the gas density in the compression chamber to the gas density in the expansion chamber at time = 0.

Table 1
SPHC Test Case Conditions

No. Of Particles	100
Gas	Air
Initial Gas Density	1.004 kg/m^3
Compression Ratio	10
Temperature	300 K
Shock Tube Length	1.0 cm
Diaphragm Location	0.4 cm
Smoothing Length	0.015
Art. Visc. Parameters α β	1.0 1.0

The results of the SPHC shock tube test case are displayed in Figures 3a and 3b for t = 0 and t = $1 x 10^{-6}$ time units respectively. The units for time are not reported by the code. Also, SPHC does not explicitly calculate pressure values for output so only density profiles are plotted. In Figure 3a a

slight deviation from a vertical slope in density occurs at the diaphragm location. This results from the resolution capability of the code for finite numbers of particles. Increasing the number of particles used in the computation moves the density profile closer to the expected vertical slope at the diaphragm location.

Figure 3b displays the density profile at 1×10^{-6} time units after the diaphragm is shattered. It exhibits the same qualitative density profile as that seen in Figure 1. However, the changes in density at both the contact discontinuity and the shock front are smeared and extend over a smoothing length range of $\sim 5h$ and $\sim 3h$ respectively. Increasing the number of
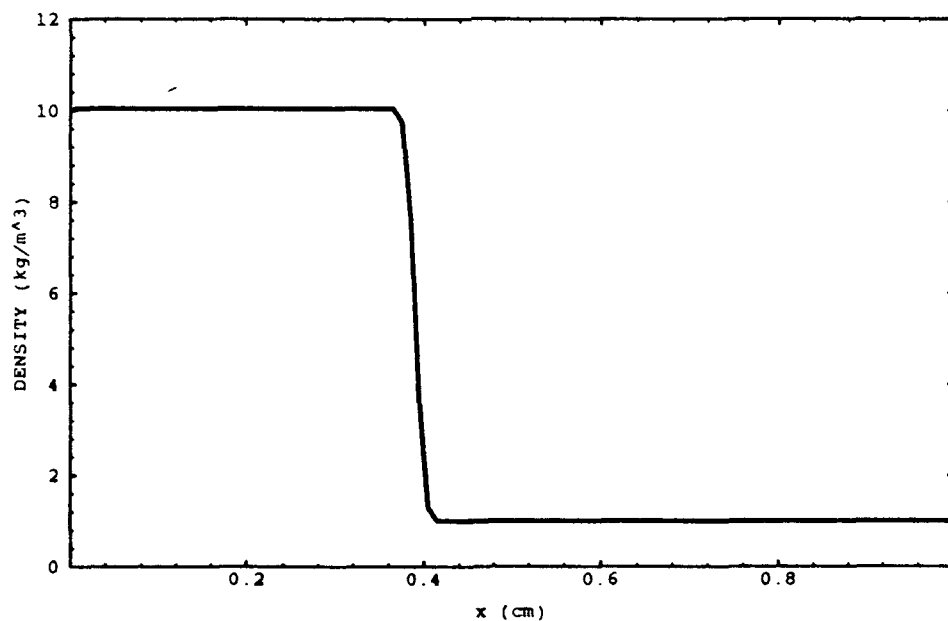

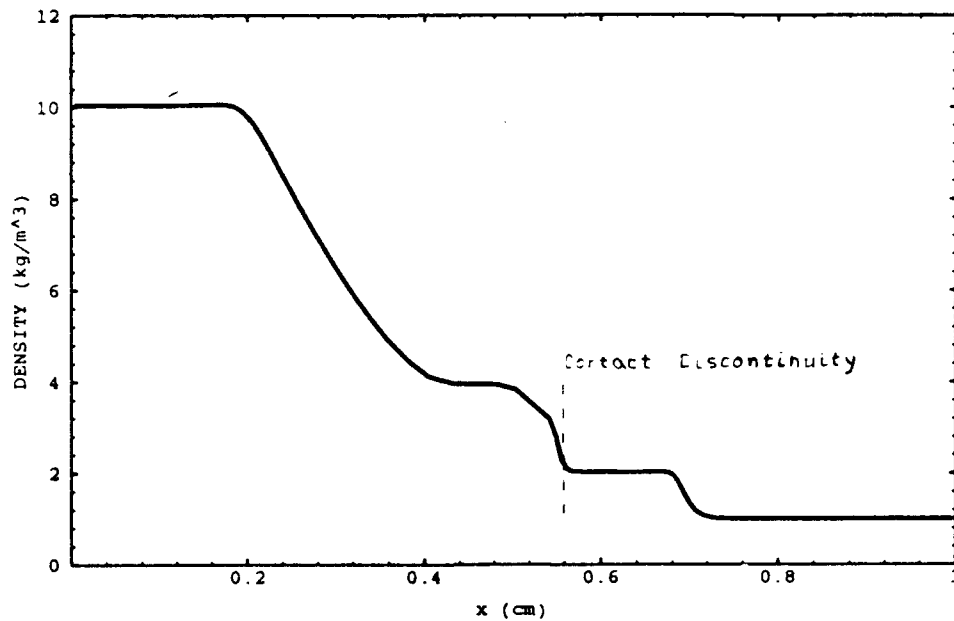Figure 3. a) SPH shock tube test, 100 particles, $h = 0.015$, t = 0

Figure 3.   b) SPH shock tube test, 100 particles,
$h = 0.015$, $t = 1 \times 10^{-6}$

particles from 100 to 500 much appears to improve the resolution
as seen in Figure 4. Now, the changes in density at the contact
discontinuity and shock front are quite sharp and only a slight
rounding is apparent at the contact discontinuity.   However,
increasing the number of particles by a factor of 5 resulted
in a reduction of h by 1/5.   The density is still smeared over
the same h at both the shock front and contact discontinuity.
The only difference is that the smoothing length is reduced.
The artificial viscosity parameters must be varied to reduce
smearing of the shock front and contact discontinuity.

It is apparent that the 1-D shock tube version of SPHC produces results that qualitatively agree with theoretical predictions and an exact solution to a standard Riemann shock tube problem. Now that confidence in the SPH code is established, shock tube results of the Lagrangian hydrodynamic code will be analyzed in a similar fashion.
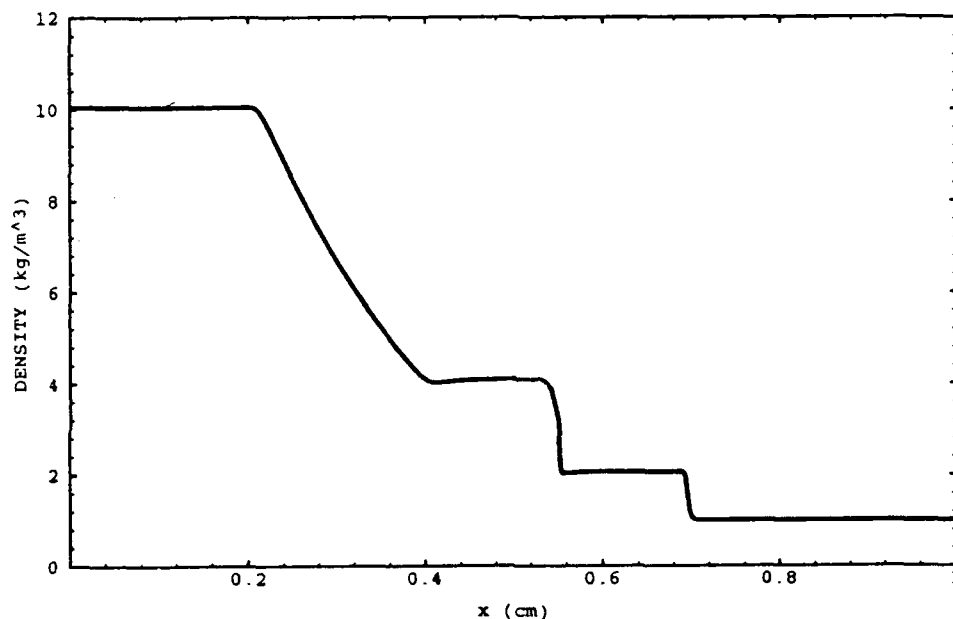

Figure 4. SPH shock tube test, 500 Particles,
h = 0.003, t = 1×10^{-6}

3.4 Lagrangian Shock Tube Validation

A 1-D shock tube test case was run using a modified version of a Lagrangian hydrodynamic algorithm developed by Bridgman (18). The test case was run at the same initial conditions as those listed in Table 1 except 200 computational cells were used instead of 100 particles and the artificial viscosity

18

parameter $\alpha = 2$. Thermal equilibrium was assumed to exist between the gases on both sides of the diaphragm. This assumption will continue to be applied to all test cases in this study. One advantage of the Lagrangian hydrocode over SPHC is that it explicitly calculates values of pressure for output.

Figures 5 and 6 show the pressure profiles at times 0 and $6 x 10^{-4}$ seconds, respectively, after the diaphragm is shattered. These results almost perfectly model the predicted pressure behavior displayed in Figures 2b and 2c. There is a slight dip in pressure followed by some minor oscillations at the tail of the rarefaction wave in Figure 6. This behavior has been seen in other numerical methods incorporating an artificial viscosity term (4:382). The density profile also displays some oscillatory behavior as seen in Figure 7. The density changes at the contact discontinuity and shock front are sharp and almost vertical in slope. A small smearing of the contact discontinuity and shock front will occur due to the artificial viscosity.

The Lagrangian hydrocode showed excellent agreement with predicted behavior for both density and pressure profiles. Confidence in the ability of both codes to produce credible results for shock tube problems has been established.
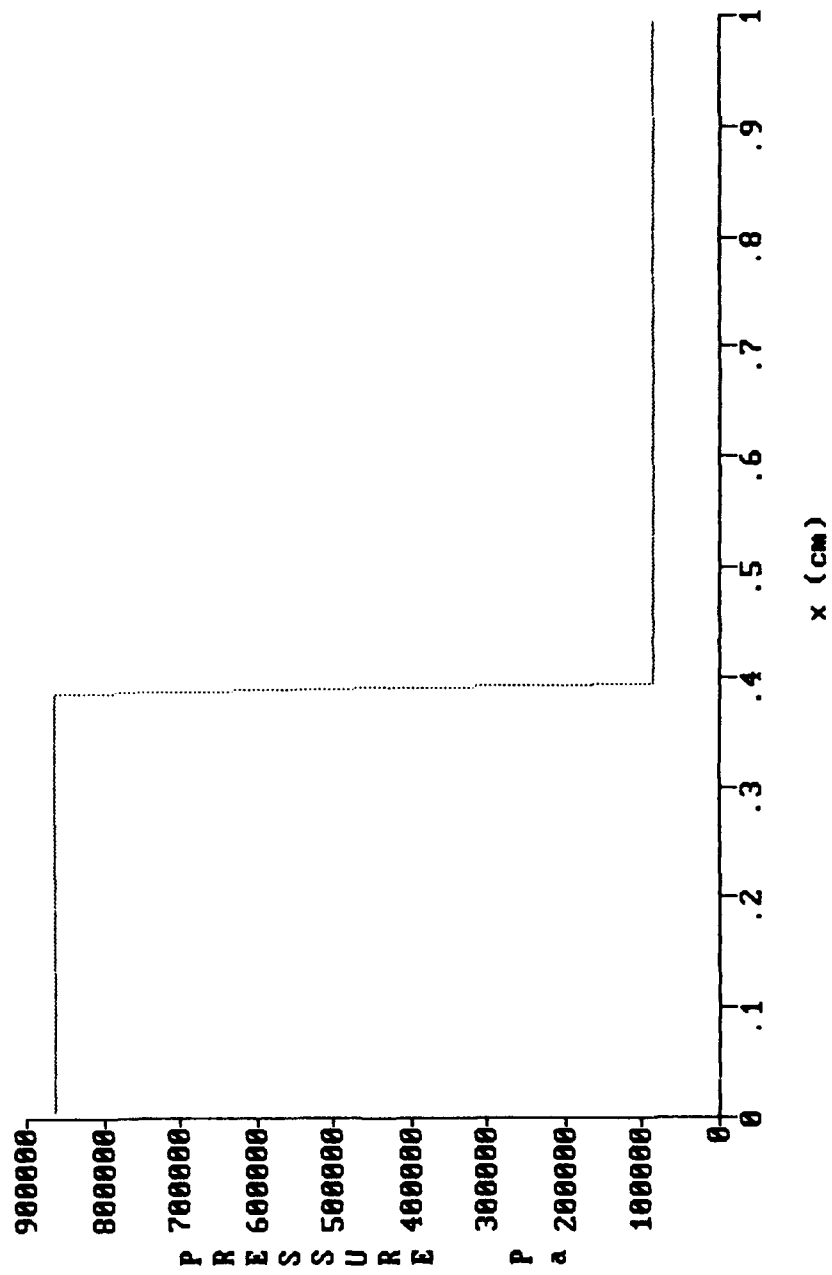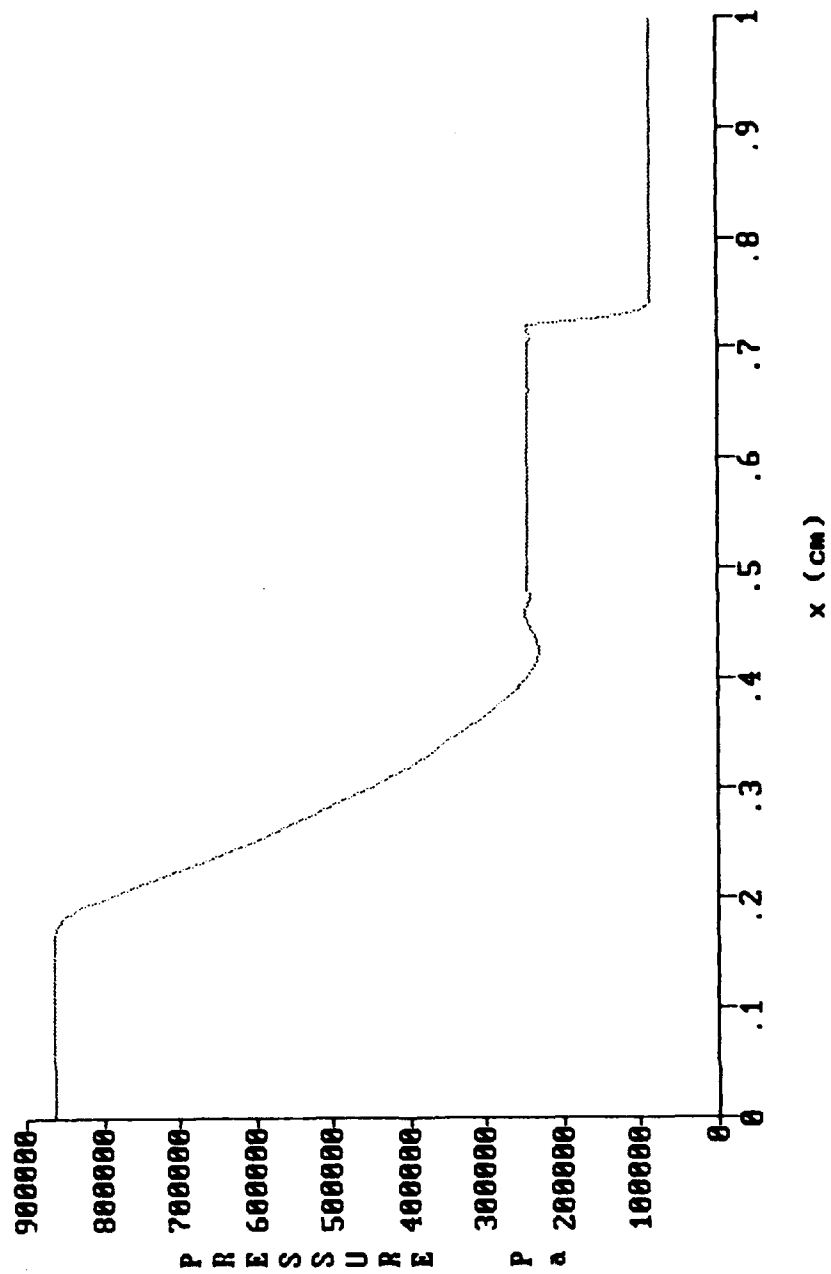
Figure 5.   Hydrocode pressure profile, 200 cells, t = 0

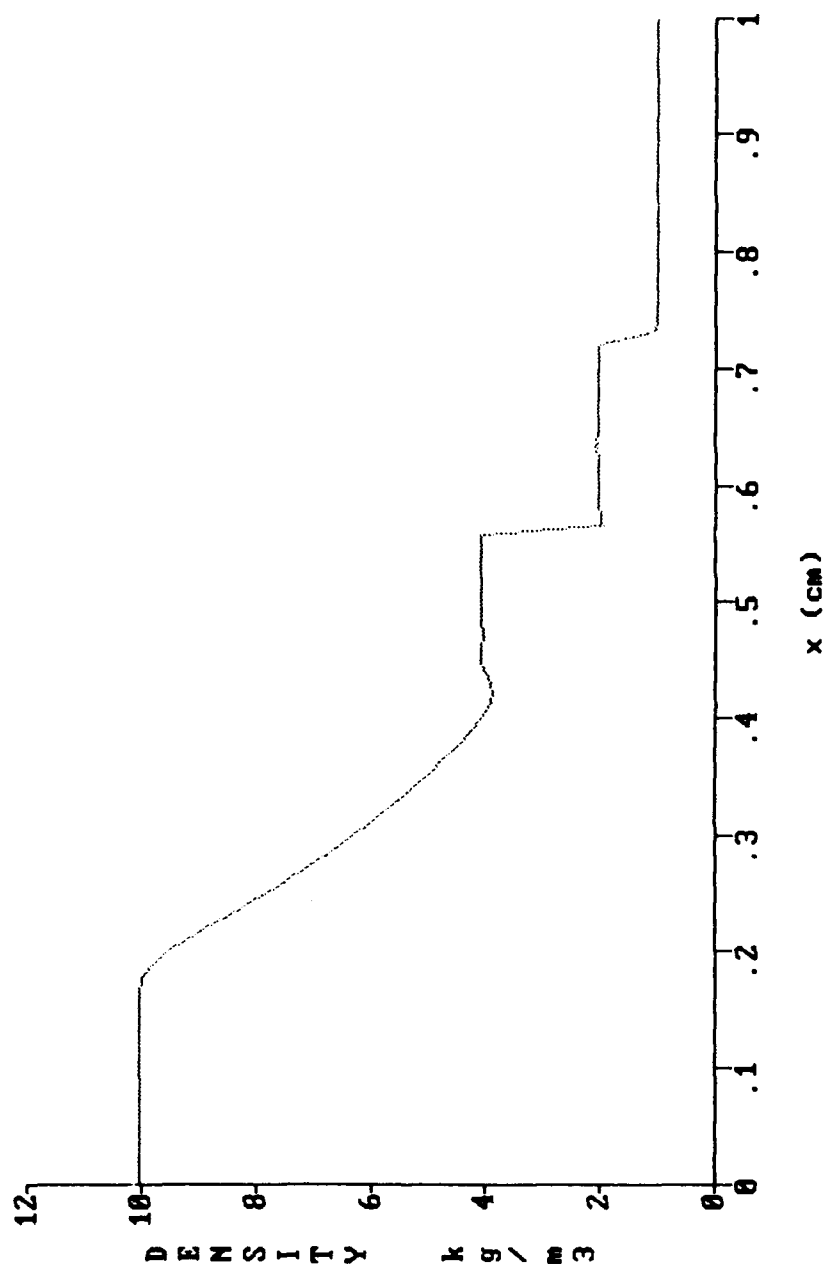Figure 6. Hydrocode pressure profile, $t = 6 \times 10^{-4}$ sec

Figure 7. Hydrocode density profile, $t = 6x10^{-4}$sec

IV. <u>Results</u>

A compression ratio, η, of 10 is not typical of the magnitudes at which actual shock tube tests are run. The Defense Nuclear Agency (DNA) is developing a Large Blast/Thermal Simulator (LB/TS) with a driver gas at a pressure of 1740 psig (19). Ambient pressure is 14.7 psig, so this equates to η ≈ 120. The following shock tube test cases were run at η = 100 to better simulate actual test conditions.

Comparisons between SPHC and the Lagrangian hydrocode were made when prominent features such as the shock front reached the same spatial position for both codes. Time comparisons could not be made since the Lagrangian hydrocode had times approximately 500 times greater than SPHC. For example, the shock front reached x = 0.8 cm at t = 0.5 msec for the hydrocode whereas the SPHC code reached the same position at $t = 1 x 10^{-6}$ time units. SPHC does not provide the units for time in the output nor did the users manual specify the units.

4.1 <u>Resolution of Density Profiles</u>

Figures 8a, b and c show the density profiles for SPHC using 100, 200 and 500 particles, respectively. As expected the resolution of the density change at both the contact discontinuity and shock front improve with increasing number of particles. However, an anomalous spike occurs at the contact discontinuity that was not seen in the SPHC results at η = 10.
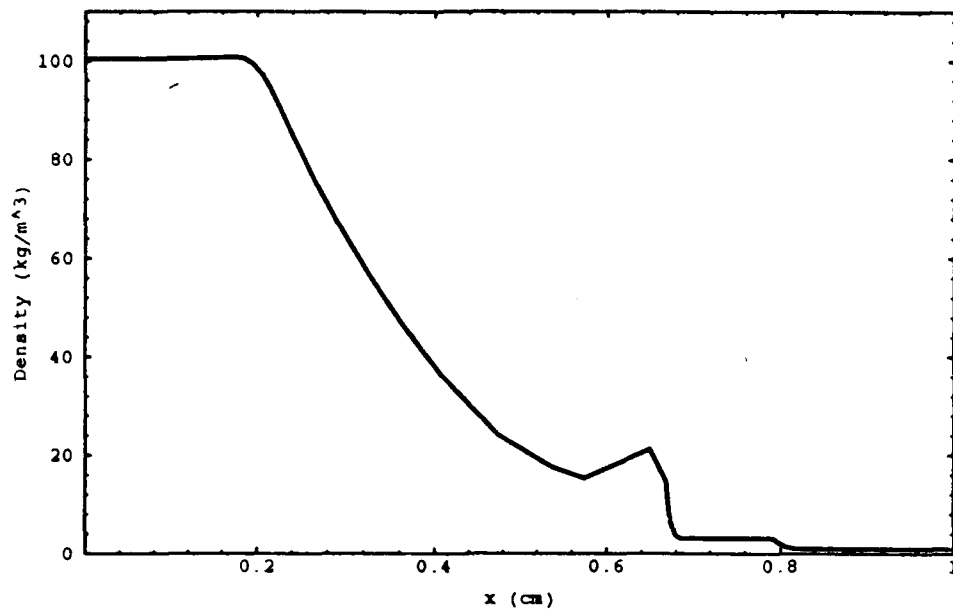
a)
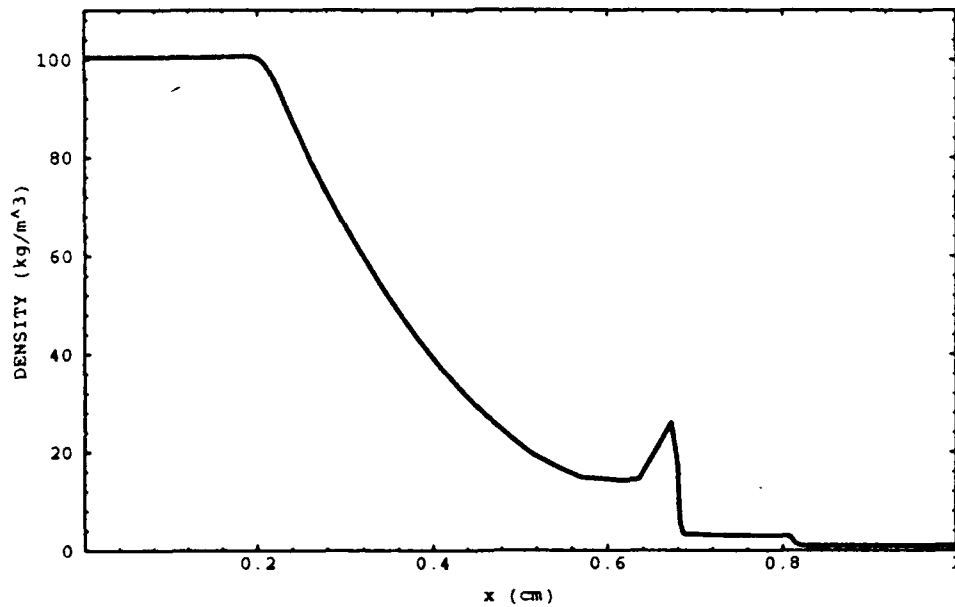
b)

Figure 8.   Density profiles for SPH at $\eta = 100$ using
a) 100 and b) 200 particles
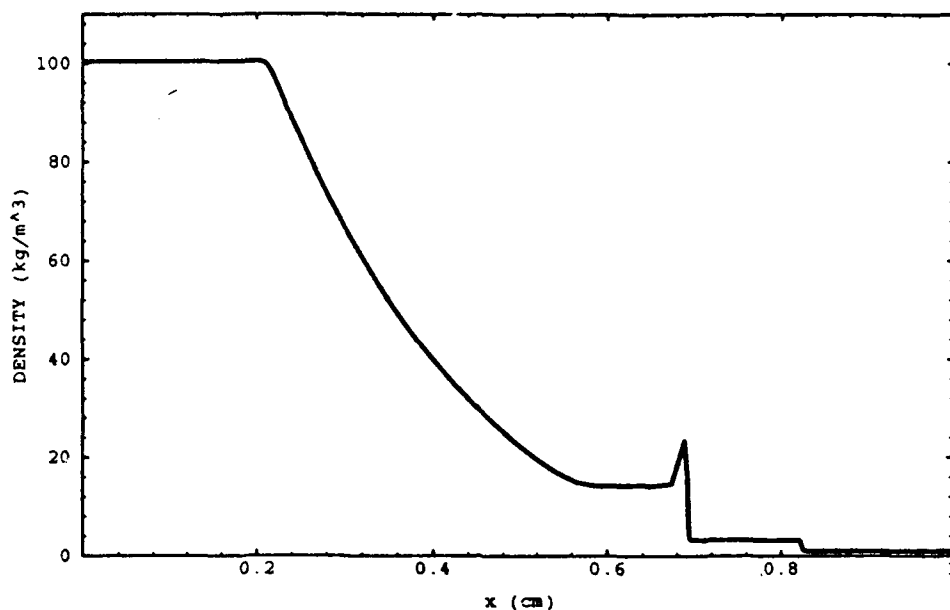
Figure 8. c) Density profile for SPH using 500 particles

This feature was not reported in the references on shock simulation by SPH (4,10) since they conducted the shock tube tests at $\eta = 4$.

The spike in density to the left of the contact discontinuity may result from a piling up of particles in this high density region. Stellingwerf (11) reports that SPH codes were normally limited to a density contrast of about a factor of 3 due to fixed-size particles. The density contrast across the contact discontinuity is a factor of 5. SPHC has a particle division/recombination option which is supposed to maintain resolution in regions of high density contrast. This option was not used in this test case due to time limitations.

25

Figures 9a, b and c show the density profiles for the Lagrangian hydrocode using 100, 400 and 800 cells, respectively. The hydrocode does a poor job of resolving the contact discontinuity and the shock front using 100 cells as seen in Figure 9a. Increasing the number of cells to 400 dramatically improves the resolution although a small dip in density occurs at the tail of the rarefaction wave as seen in earlier results. Another increase to 800 cells results in a slight improvement in the density dip. As in the previous section, an artificial viscosity parameter of $\alpha = 2$ was used.
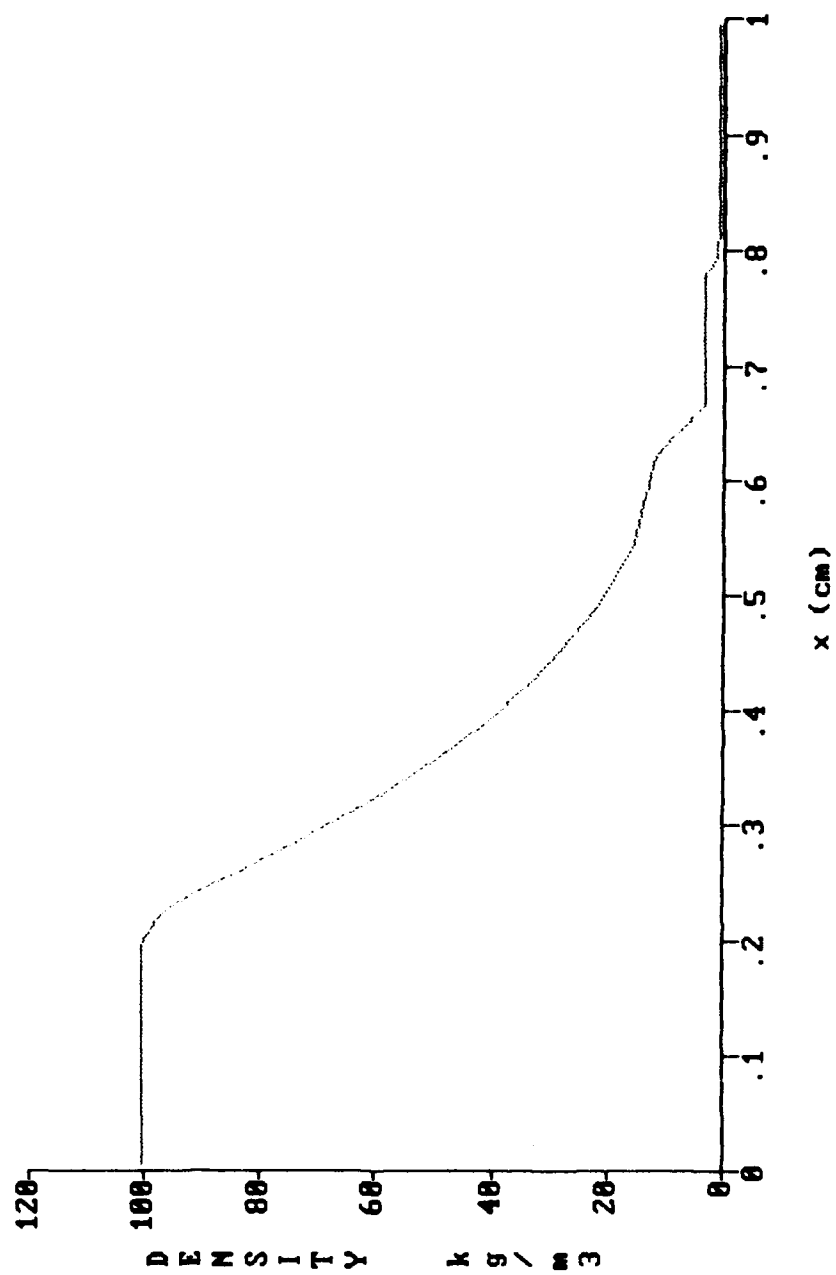
Figure 9. a) Density profile for hydrocode at η = 100
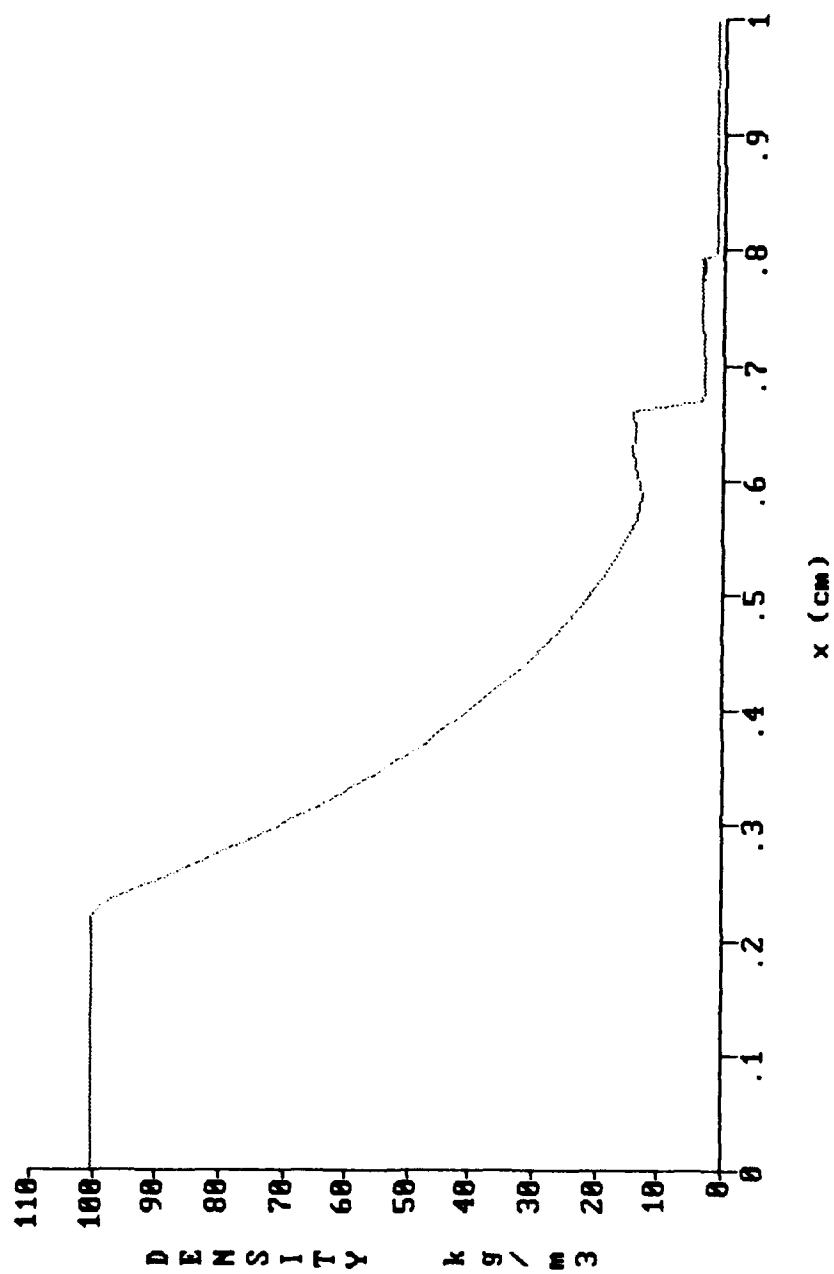using 100 cells

Figure 9. b) Density profile for hydrocode at $\eta = 100$
using 400 cells
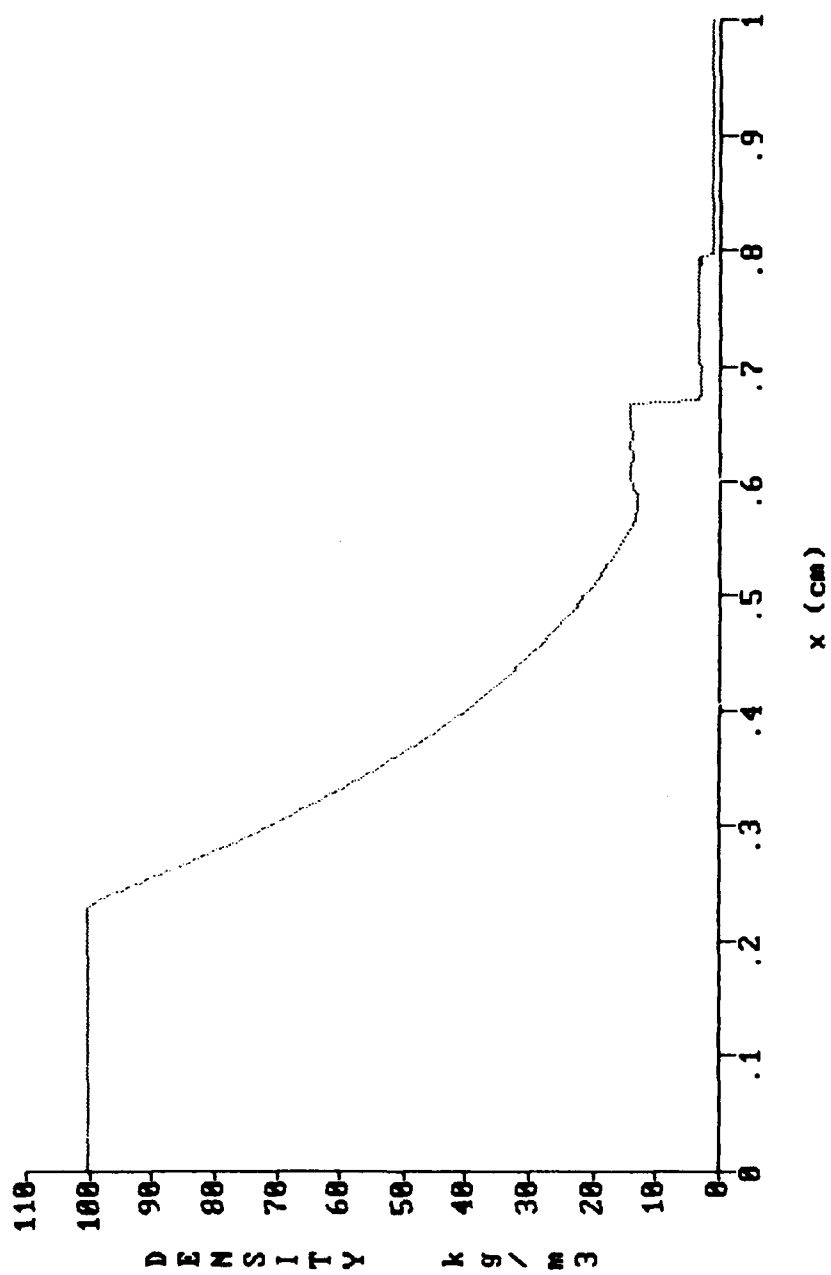
Figure 9.   c) Density profile for hydrocode at $\eta = 100$
using 800 cells

4.2 Run Time Scaling

Computation times for individual runs for both SPHC and the Lagrangian hydrocode are listed in Table 2.

Table 2
Run Times for SPHC & Lagrangian Hydrocode

SPHC a		Lagrangian Hydrocode b	
# particles	run time (min)	# cells	run time (min)
50	3	100	1.3
100	9	200	5.1
200	22	400	20
500	93	800	82

a Sun SPARC2 workstation
b 386SX, 16 MHz PC

The 500 particle SPHC run and the 400 cell hydrocode run give qualitatively comparable resolution of the density profile. However, SPHC requires over four times the computation time. The references on SPH methods support this finding and only claim that SPH schemes are computationally superior in 2- and 3-D geometries (7). Computation times between SPHC and the hydrocode may be even greater since SPHC was run on a Sun SPARC2 workstation while the hydrocode was run on a 386-SX, 16 MHz PC. The Sun is an estimated 5 - 10 times faster than

the PC. Therefore, a conservative estimate is that the Lagrangian hydrocode is running twenty times faster than SPHC for comparable resolution.

Computation time for the hydrocode increases by a factor of four for every doubling of the number of cells. This equates to run time scaling of $O(N^2)$. The literature (9, 20) predicts that SPH methods using a hierarchical tree-structured technique for force calculations between N particles will scale as $O(N\log N)$. Figure 10 shows that the SPHC run times are $N\log N < t < N^2$.

The Lagrangian hydrocode proved to require less computation time than SPHC for $N \leq 500$. However, N^2 scaling has a steeper slope than $N\log N$ scaling, so for problems involving $N - 10^3 - 10^4$, the Lagrangian hydrocode becomes computationally more expensive.
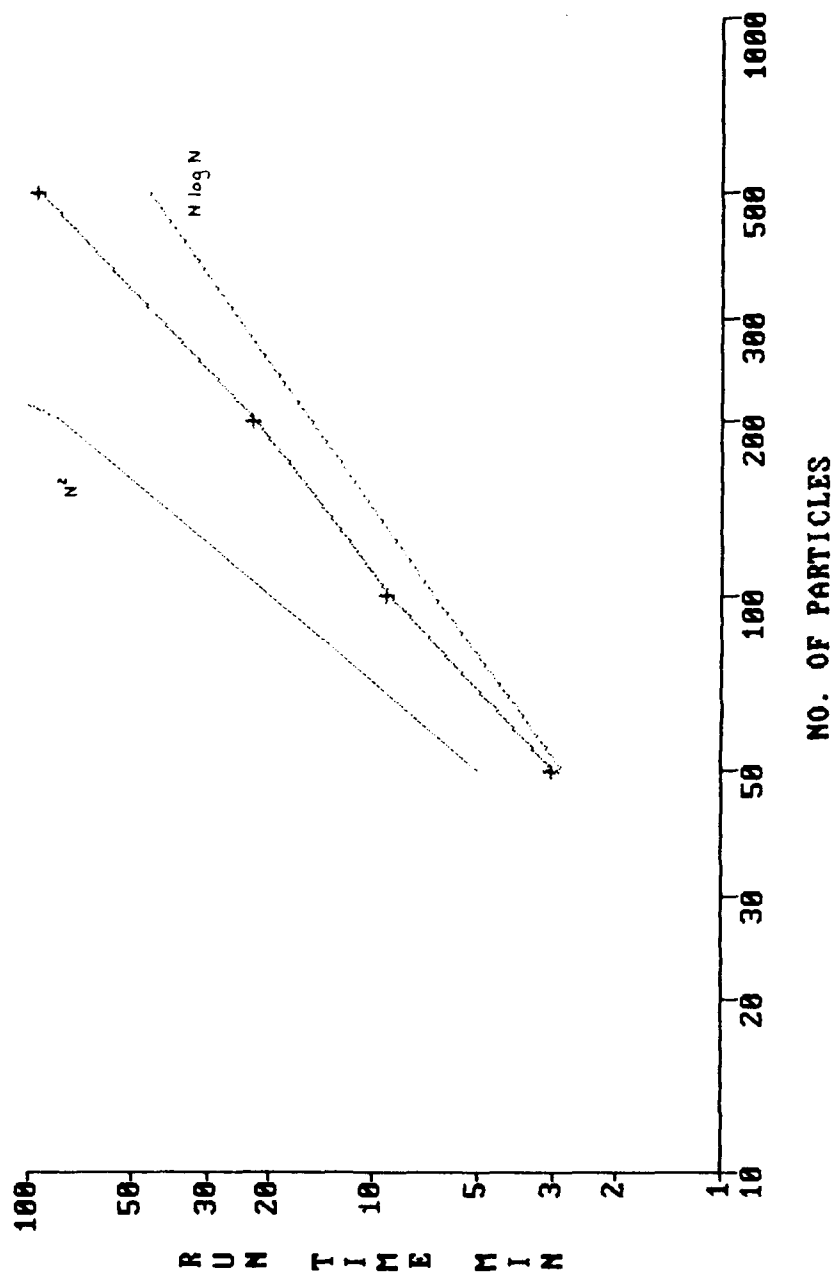
Figure   .   SPHC run time scaling

V. Analysis of SPHC

A discussion of the unique features of the SPH code is presented below. Also presented are the problems encountered in evaluating the code and the change in scope of the study.

5.1 Smooth Particle Hydrodynamic Code (SPHC)

Mission Research Corporation (MRC) of Albuquerque, NM has developed a benchmark SPH code, SPHC, as a testing arena for the SPH technique. What sets this code apart from earlier pioneering efforts in SPH is its emphasis on simulating non-astrophysical problems. SPHC incorporates many features to overcome the deficiencies found in earlier codes that limited their use primarily to the astrophysics realm.

5.1.1 SPHC Features. SPHC addresses the problems of run time scaling, limited density range, fluid interpenetration and treatment of boundaries (11:2-4).

1) Run time scaling. To reduce computational requirements, SPHC uses a hierarchical tree scheme for neighbor location which ensures scaling of $N \log N$ instead of N^2 where N is the number of particles.

2) Density range. Original SPH methods used fixed size particles which limited density contrast to a factor of 3. MRC uses variable size particles and a new technique that allows particle division in low density regions to maintain resolution.

3) Interpenetration. A specialized tensor artificial viscosity (10:591-595) is used to address the problem of particle streaming at interfaces. This problem is especially severe in shocks and collisions.

4) Boundaries. SPH is a gridless technique and boundaries cannot be identified with particular particles. Therefore, SPHC incorporates a wall boundary based on terms normally dropped in the integration-by-parts step of converting equations to numerical format. A ghost particle boundary is also used for reflecting and periodic cases.

In addition to the above, SPHC has several other new features. It is written in C and can be run on Cray, Sun and even MS-DOS environments. SPHC runs in 1-, 2-, or 3-dimension modes as well as in spherical and cylindrical geometries. MRC has also included new models to treat electron thermal conduction, single group radiation diffusion, laser deposition and inertial confinement fusion (ICF) physics.

5.2 Code Evaluation.

SPHC is reported by Stellingwerf (11:4) to have been "thoroughly and carefully tested against analytic solutions and other codes on rarefaction, shock tube, blast wave, exponential atmosphere, and collisions problems." Two factors made SPHC particularly attractive for this study: 1) standard test problems have

already been set up and executed for 2- and 3-D blast wave calculations and 2) SPH methods are often computationally superior to mesh-based methods for 2- and 3-D applications.

The initial objectives, therefore, of this study were twofold. First, scope the computational limits of this particle method and evaluate its potential as a simulation tool for studying blast wave phenomena. Second, apply the code to the problem of shock wave stagnation/reflection in a corner. Unfortunately, the initial objectives could not be achieved due to unforeseen problems with the code. This will be discussed in the following paragraphs.

The SPHC production code is not a general purpose code. Different hydrodynamic problems such as rarefaction, shock tube or blast wave cannot be executed using the same main module code, sphc.c. Although all use the same underlying physics, MRC has developed individual SPHC versions for each test case. However, setup menus are included during program initialization to allow adjustment of parameters such as number of time steps, boundary types, physics models and equation of state parameters. Making changes to the test problem con- figuration beyond available parameter adjustments requires modifying the module setup file, sph_init.c, and recompiling the code.

The SPHC version employed in this study is a version of the standard Riemann shock tube test case in one dimension with Cartesian geometry. Executing the program required

compiling the main module code sphc.c with the 1-D shock tube setup file sph_init.c. While the program performed as expected for the shock-tube test case (to be discussed later), the rarefaction and 2-D blast wave setup files did not successfully compile with this version of SPHC. The code for these two setup files came from the SPHC user manual that accompanied the main module code. Failure of these two test cases to execute with the available version of the SPHC code proved conclusively that this version of the SPHC code was applicable only for performing 1-D shock tube tests and inadequate for evaluation of 2- and 3-D blast wave problems.

At this point, obtaining the correct version of SPHC for blast wave simulation was not pursued because it required further delay of the effort. Second, and more importantly, the setup file for the blast wave test case required code modification to deal with the configurations of interest such as shock wave stagnation/amplification in a corner. The expertise was not readily available to perform this task.

VI. Conclusions and Recommendations

A smooth particle hydrodynamic code was evaluated using shock tube simulation as a test case. A summary of conclusions from the results presented in this study and recommendations for further investigation are discussed in the following two sections.

6.1 Conclusions

SPHC displayed the capability to model shocks accurately at low shock strengths. This confirms previous reports in the literature. At compression ratios of interest to the weapons effects community the code produced an anomalous spike in the density profile at the contact discontinuity. The literature has not reported such behavior since shock simulations have been performed at low shock strengths. SPHC may have the ability to eliminate this behavior by use of a particle division/recombination method, but this was not confirmed in this study. The density profiles generated by SPHC did not exhibit the dip in density and oscillations at the tail of the rarefaction wave as did the Lagrangian hydrocode.

A drawback of the code is that values of pressure are not explicitly calculated as an output variable. Temperature and density values are calculated. Pressure could therefore be calculated for gases obeying the ideal gas law. Another

drawback is that the code is problem specific. Each version of SPHC is dedicated only to one problem such as rarefaction, shock tube, blast wave, etc.

Run times for SPHC scale between $N\log N$ and N^2. The Lagrangian hydrocode scaled $O(N^2)$. Computation times for SPHC were four times greater than for the hydrocode for $N \leq 500$ particles to achieve similar resolution and may actually be greater by a factor of twenty if the codes are run on the same computer. However, for problems involving a larger number of particles, run times for the hydrocode scale at a steeper rate and will exceed run times for SPHC.

6.2 Recommendations

Although the evaluation of the SPH method was preliminary in nature, the technique itself merits further study as does the MRC SPH code. SPH methods have only been in existence for a relatively short ten year span and only recently have they been seriously applied to non-astrophysics problems. The ability to handle complex flowfields without mesh entanglement and superior computational performance in two- and three-dimensions make particle methods a prime candidate for multi-dimensional blast wave calculations.

Specific recommendations for further study of SPHC are:

1) a study of the 2- and 3-D blast wave and fireball test cases performed by MRC,

2) compare SPHC blast wave test case to an existing blast wave code using the same computer for run time comparisons,

3) evaluate the inertial confinement fusion version of SPHC for credibility against recent ICF work, and

4) investigate the various physics options available for program execution such as thermal and radiation diffusion options.

Bibliography

1. Dolan, Philip J. and Samuel Glasstone. <u>The Effects of Nuclear Weapons</u> (Third Edition). Washington: Government Printing Office, 1977.

2. Eisenbud, Merril. <u>Environmental Radioactivity</u> (Third Edition). New York: Academic Press, Inc., 1987.

3. Lucy, L. B. "A Numerical Approach to Testing the Fission Hypothesis," <u>Astronomy Journal</u>, 82: 1013-1024 (1977).

4. Gingold, R. A. and J. J. Monaghan. "Shock Simulation by the Particle Method SPH," <u>Journal of Computational Physics</u>, 52: 374-389 (1983).

5. Benz, W., W. L. Slattery, and A. G. W. Cameron. <u>Icarus</u>, 66: 515 (1986).

6. Benz, W. and J. G. Hills. "Three-Dimensional Hydrodynamical Simulations of Stellar Collisions," <u>The Astrophysical Journal</u>, 323: 614-628 (December 1987).

7. Loewenstein, Michael and William G. Mathews. "Adiabatic Particle Hydrodynamics in Three Dimensions," <u>Journal of Computational Physics</u>, 62: 414-428 (1986).

8. Benz, W., <u>et al</u>. "Dynamic Mass Exchange in Doubly Degenerate Binaries," <u>The Astrophysical Journal</u>, 348: 647-667 (January 1990).

9. Appel, Andrew W. "An Efficient Program for Many-Body Simulation," <u>SIAM Journal on Scientific and Statistical Computing</u>, 6: 85-103 (January 1985).

10. Lattanzio, J. C., <u>et al</u>. "Controlling Penetration," <u>SIAM Journal on Scientific and Statistical Computing</u>, 7: 591-598 (April 1986).

11. Stellingwerf, Robert F. "Smooth Particle Hydrodynamics," <u>Lecture Notes in Physics: Free-Lagrange Conference Proceedings, </u> (1990).

12. Monaghan, J. J. "Why Particle Methods Work," <u>SIAM Journal on Scientific and Statistical Computing</u>, 3: 422-433 (December 1982).

13. Campbell, P. M. <u>Some New Algorithms for Boundary Value Problems in Smooth Particle Hydrodynamics</u>. DNA-TR-88-286. Washington: Defense Nuclear Agency, June 1989. (AD-A211 728)

14. Wright, John K. <u>Shock Tubes</u>. Methuen's Monographs on Physical Subjects. New York: John Wiley & Sons, Inc., 1961.

15. Roe, P. L. "Approximate Riemann Solvers, Parameter Vectors, and Difference Schemes," <u>Journal of Computational Physics</u>, **43**: 357-372 (1981).

16. Esser, B. and Gronig, H. "Equilibrium Shock Tube Flow of Real Gases," <u>Shock Tubes and Waves</u>, Proceedings of the 16th International Symposium on Shock Tubes and Waves, Aachen, West Germany, VCH Publishers, 1988.

17. Sod, G. A. <u>Journal of Computational Physics</u>, 27: 1 (1978).

18. Bridgman, C. J. Class Notes in NENG 631, Prompt Effects of Nuclear Weapons. School of Engineering, Air Force Institute of Technology (AU), Wright-Patterson AFB OH, March - May 1991.

19. Mason, Gregory P. "Development of a Pebble-Bed Liquid Nitrogen Evaporator and Superheater for the Scaled Large Blast/Thermal Simulator (LB/TS) Facility," <u>MABS 11: Proceedings of the 11th International Symposium on Military Applications of Blast Simulation</u>, Albuquerque NM, Sept 1989.

20. Barnes, Josh and Hut, Piet. "A Hierarchical O(N log N) Force-Calculation Algorithm," <u>Nature</u>, Vol 324 (December 1986).

Vita

Luke Lorang was born on March 20, 1964 in Grand Forks, North Dakota. He attended O'Gorman High School in Sioux Falls, South Dakota and graduated in May of 1981. Luke obtained his Bachelor of Science degree in Chemical Engineering at the South Dakota School of Mines and Technology and graduated with highest honors in May of 1985. He entered the Air Force Officer Training School in July of 1986 and graduated as First Honor Graduate in October of the same year. His first assignment was at the Rome Air Development Center (RADC) at Griffiss AFB NY, where he was lead engineer for materials R&D and reliability assessment of organic materials used in military microelectronics. After four years at RADC he attended the Air Force Institute of Technology at Wright-Patterson AFB OH to complete a Master of Science degree in Nuclear Engineering.

Permanent Address: 2905 S. Marion Road

Sioux Falls, South Dakota 57106

(605) 361-3634